2023 62nd IEEE Conference on Decision and Control (CDC)
December 13-15, 2023. Marina Bay Sands, Singapore

Exploring CAV-based traffic control for improving traffic conditions in the face of bottlenecks

Suyash C. Vishnoi[†,‡], Junyi Ji[††], MirSaleh Bahavarnia[††], Yuhang Zhang[††], Ahmad F. Taha[††], Christian G. Claudel[†], and Daniel B. Work[††]

***Abstract*— This work investigates traffic control via controlled connected and automated vehicles (CAVs) using novel controllers derived from the linear-quadratic regulator (LQR) theory. CAV-platoons are modeled as moving bottlenecks impacting the surrounding traffic with their speeds as control inputs. An iterative controller algorithm based on the LQR theory is proposed along with a variant that allows for penalizing abrupt changes in platoon speeds. The controllers use the Lighthill-Whitham-Richards (LWR) model implemented using an extended cell transmission model (CTM) which considers the capacity drop phenomenon for a realistic representation of traffic in congestion. The effectiveness of the proposed traffic control algorithms is tested using a traffic control example and compared with existing proportional-integral (PI)- and model predictive control (MPC)- based controllers from the literature. A case study using the TransModeler traffic microsimulation software is conducted to test the usability of the proposed controller in a realistic setting. It is observed that the proposed controller works well in both settings to mitigate the impact of the jam caused by a fixed bottleneck. The computation time required by the controller is also small making it suitable for real-time control.**

***Index Terms*— Traffic control, Moving bottleneck control, Connected and autonomous vehicles, Linear-quadratic regulator.**

I. Introduction

The advent of connected and autonomous vehicle (CAV) technology has led to the opening of unforeseen avenues in the field of traffic control [1]. Compared to fixed actuators such as variable speed limit (VSL) signs [2] and boundary flow controllers [3], control using CAVs offers greater flexibility as it allows actuators to move in space in a desired manner, therefore, allowing them to be present at desired locations at desired times. In addition to that, using CAVs is relatively cheaper than using fixed actuators which need to be specifically deployed only for the single purpose of traffic control whereas CAVs can be used for other applications like sensing. Also, CAV-based control can be effective in communities with low compliance rates to traditional fixed actuators as their physical presence ahead of drivers would make it impossible for them to avoid the control.

Given the advantages mentioned above, it is essential to explore this potential of traffic control via CAVs by developing new control methodologies that treat CAVs as moving actuators. In this work, we consider the problem of maximizing the mean speed (MS) of traffic through traffic jam dissipation by controlling the speed of CAV-platoons that act as rolling roadblocks blocking the entire flow of traffic at their location. The main focus of this work is on proposing and investigating a new controller implementation for this problem in a linear-quadratic regulator (LQR) framework which has not been explored in the literature and comparing it with existing approaches from the literature in terms of performance and computational tractability for real-time control.

Several studies in the past decade have considered the problem of moving bottleneck control of traffic to improve traffic flow. In [4], the authors have proposed a proportional-integral (PI)-type feedback regulator to perform traffic control by controlling the speed of CAV-platoons. PI-based controllers can produce the desired improvements in traffic flow when coupled with certain arbitrary constraints on vehicle speeds but do not generally guarantee optimal control. In [5], the authors propose a model predictive control (MPC)-based speed control algorithm to control the traffic via CAV-platoons subject to the travel time reduction. Their proposed speed control algorithm is optimal but requires solving a nonlinear optimization problem at each time-step which is highly time-consuming, especially for large networks with several links and junctions, as it requires performing the simulation several times, and therefore can be infeasible for real-time control. Note that here we are only interested in studies that use CAV-platoons as moving bottlenecks for traffic control. Readers are referred to [1] for an extensive review of other use cases associated with CAVs in the realm of traffic control.

To overcome the time requirement issue of the MPC-based control algorithm and make a balance between the quality of the speed control algorithm and its computational requirements, we formulate the traffic control problem in the form of an LQR-based optimization problem which regulates the states around an equilibrium point while utilizing the structure of the state-space dynamics of the system. In this work, we utilize the macroscopic traffic model presented in [5] which incorporates the capacity drop phenomenon as it allows for realistic control. We also present a microscopic traffic simulation-based case study that tests the usability of the proposed controller in the real world. Such a study is absent in [4], [5] which only consider macroscopic simulation.

Given the main research gap in this area is the absence of an optimal controller offering fast computation of controls for real-time moving bottleneck control of traffic and the absence of a study on the moving bottleneck controllers under realistic settings, the present study makes the following contributions:

- An LQR-based controller design with macroscopic model dynamics is proposed to control the speeds of CAV-platoons allowing for mitigation of the effect of jam-forming

[†]Department of Civil, Architectural, and Environmental Engineering, The University of Texas at Austin, 301 E. Dean Keeton St. Stop C1700, Austin, TX 78712. [††]Department of Civil and Environmental Engineering, Vanderbilt University, 2201 West End Ave, Nashville, TN 37235. [‡]Corresponding author. Emails: scvishnoi@utexas.edu, junyi.ji@vanderbilt.edu, mirsaleh.bahavarnia@vanderbilt.edu, yuhang.zhang.1@vanderbilt.edu, ahmad.taha@vanderbilt.edu, christian.claudel@utexas.edu, and dan.work@vanderbilt.edu. This work is partially supported by the National Science Foundation (NSF) under Grants 1636154, 1728629, 1739964, 1917056, 2135579, 2152928, 2152450, and USDOT CAMMSE.

bottlenecks in the traffic stream. Also, the impact of various parameters of the LQR-based controller is investigated with respect to its performance in solving the given problem.

- A variant of the LQR-based controller allowing for a penalty on large changes in control inputs over consecutive time-steps is developed and shown to reduce the magnitude of fluctuations in the controlled speeds allowing for safe and realistic control.
- We present a comparison of the proposed LQR-based controllers with existing MPC-based [5] and PI-based [4] controllers in terms of computational tractability and performance using macroscopic simulation.
- The performance of the proposed LQR-based controller is further investigated using a microscopic traffic simulation setup to assess its applicability and utility under realistic settings of traffic flow.

The remainder of the paper is organized as follows: Section II describes the traffic dynamics model used in this work. The problem statement with the LQR-based solution scheme and algorithms is presented in Section III. Section IV analyzes the proposed approach in a macroscopic setting, and compares it with existing approaches from the literature. Section V further analyzes the proposed approach with the help of a microsimulation-based case study. The paper is concluded with Section VI which also proposes directions for future work.

Notations: We denote the vectors and matrices by lowercase and uppercase bold symbols, respectively. The set of m-dimensional real-valued vectors and $n \times p$ real-valued matrices are respectively denoted by $\mathbb{R}^m$ and $\mathbb{R}^{n\times p}$. The identity matrix of dimension q is represented by $\boldsymbol{I}_q$. The set-theoretical minimum and maximum operators are denoted by $\min$ and $\max$, respectively.

II. Traffic Dynamics Model

We present the state-space formulation for the traffic dynamics model considered in this work. The flow of traffic across a highway stretch with no on-ramps or off-ramps is modeled using the first-order LWR model [6], [7] while accounting for the capacity drop phenomenon [8]. The model is implemented using a Godunov scheme [9] which is proposed previously in [5] and is an extension of the classical Cell Transmission Model (CTM) implementation [10]. Within this, the highway stretch is divided into N_L segments of equal length L (km) and the time horizon is divided into N_T smaller duration of T (sec) each such that the Courant-Friedrichs-Lewy (CFL) condition [11]: $T \leq L/v_f$ is satisfied where v_f refers to the free-flow speed of traffic. Let N_{CAV} be the total number of controlled CAV-platoons currently on the modeled highway stretch. The traffic dynamics model is given as follows:

$$\rho_i[k+1]=\rho_i[k]+\frac{T}{L}(\phi_{i-1}(\rho_{i-1}[k],\boldsymbol{u}[k])-\phi_i(\rho_i[k],\boldsymbol{u}[k]),$$

$\forall i \in \{1,...,N_L\}$, where $\rho_i[k]$ represents the traffic density (vehicles per unit length) in Segment i at time index k, $\boldsymbol{u}[k] \in \mathbb{R}^{N_{\text{CAV}}}$ denotes the control input and is given as

$$\boldsymbol{u}[k]=\begin{bmatrix}u_1[k] & \cdots & u_{N_{\text{CAV}}}[k]\end{bmatrix}^T, \tag{1}$$

where $u_j[k], \forall j \in \{1,\dots,N_{\text{CAV}}\}$ denotes the control speed of CAV-platoon j in the traffic stream. $\phi_i(.,.)$ is the actual traffic flow (vehicles per unit time) that leaves Segment i and is given as

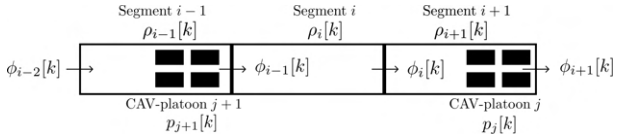

Fig. 1. Three segments of the modeled highway stretch along with two CAV-platoons and the corresponding states written underneath. Arrows indicate the direction of traffic flow.

$$\phi_i(\rho_i[k],u_j[k])=\min\{D_i(\rho_i[k],u_j[k]),S_{i+1}(\rho_{i+1}[k])\}, \tag{2}$$

assuming the CAV-platoon j is in Segment i at time index k. Figure 1 presents a schematic of the highway stretch with the two elements- Segments and CAV-platoons along with their associated states written underneath each label. Here, $D_i(\cdot,\cdot)$ and $S_{i+1}(\cdot)$ denote the traffic demand for Segment i and the supply for Segment $i+1$, respectively. Demand refers to the traffic flow wanting to leave a segment while supply refers to the traffic flow that can enter a segment. The demand and supply functions are defined using minimum functions of the state and input variables. Interested readers are referred to [12] for the exact mathematical definitions which are omitted from this paper for brevity. In the sequel, for convenience, we denote the demand, supply, and actual flow with the function names followed by the time index without mentioning the inputs required to calculate each. The position of CAV-platoon j on the highway is denoted by $p_j[k]$ where its evolution over time is given as

$$p_j[k+1]=p_j[k]+T\bar{v}_j(\rho_i[k],\rho_{i+1}[k],u_j[k]), \tag{3}$$

where $\bar{v}_j(\rho_i[k],\rho_{i+1}[k],u_j[k])$ denotes the speed of CAV-platoon j during time index k. Note that $u_j[k]$ is the control speed of the CAV-platoon or the speed prescribed to the CAV-platoon by the controller while $\bar{v}_j$ is the realized speed of the CAV-platoon which depends on the demand and supply conditions besides the control speed.

The realized speed and the corresponding final position of the CAV can be calculated according to conditions presented in [4], [12] which use the demand and supply conditions of the various segments besides the control speed. Two additional parameters namely platoon length l_j (m) and the minimum supply needed for the platoon to pass to the next segment S_{min} are also used in these calculations. The state-space equation can therefore be written as

$$\boxed{\boldsymbol{x}[k+1]=\boldsymbol{A}\boldsymbol{x}[k]+\boldsymbol{G}\boldsymbol{f}(\boldsymbol{x}[k],\boldsymbol{u}[k]),} \tag{4}$$

where the state vector $\boldsymbol{x}[k] \in \mathbb{R}^{N_L+N_{\text{CAV}}}$ is defined as

$$\boldsymbol{x}[k]=\begin{bmatrix}\rho_1[k] & \cdots & \rho_{N_L}[k] & p_1[k] & \cdots & p_{N_{\text{CAV}}}[k]\end{bmatrix}^T,$$

and the input vector $\boldsymbol{u}[k]$ is the same as in (1). Let $n_x := N_L + N_{\text{CAV}}$ be the number of states and $n_u := N_{\text{CAV}}$ be the number of inputs. The matrix $\boldsymbol{A}=\boldsymbol{I}_{n_x}$, matrix $\boldsymbol{G} \in \mathbb{R}^{n_x\times n_x}$ is a diagonal matrix representing the coefficients of the nonlinearities in the dynamics, and the vector-valued function $\boldsymbol{f}:\mathbb{R}^{n_x}\times\mathbb{R}^{n_u}\to\mathbb{R}^{n_x}$ represents the nonlinearities in the evolution of traffic density and the position of the CAVs with time which consist of differences of nested minimum functions (2) as well as CAV-platoon speeds obtained from nested conditional statements. The presence of such nonlinearity in the state space makes it necessary for control problems based on the model to utilize nonlinear optimization schemes.

III. Problem Statement and LQR-Based Traffic Control Algorithms

The underlying traffic control problem addressed in this work is defined as follows:

Problem 1. *Given the nonlinear traffic dynamics (4), control the speed of CAV-platoons entering the highway stretch at known time-steps to mitigate the adverse effects of a traffic jam formed in the middle of the stretch.*

Problem 1 can be defined in the form of an optimization problem as follows:

$$\begin{aligned} \min_{u[k]} \quad & J(\boldsymbol{x}[k],\boldsymbol{u}[k]) \\ \text{s.t.} \quad & (4) \\ & \boldsymbol{u}[k] \in \mathcal{U} \end{aligned} \tag{5}$$

where the cost function $J(\boldsymbol{x}[k], \boldsymbol{u}[k])$ is any function whose minimization ensures an improvement in the traffic conditions which can be in terms of an increase in the overall speed of traffic or a decrease in the overall congestion level on the highway in terms of traffic density. Here, the decision variables $\boldsymbol{u}[k]$ are the speeds of the CAV-platoons on the highway stretch. The essential constraints include the state-space dynamics (4) while the speeds of these platoons can also be constrained to an arbitrary set $\mathcal{U}$.

In the present work, the optimization problem (5) is formulated in the LQR optimization framework [13]. For linear systems, this results in a horizon-based optimization problem that aims to regulate the states and inputs of the system around the zero point taking into account the system dynamics over a given number of future time-steps with the help of a state-feedback law for the control input in the form $\boldsymbol{u}[k] = \boldsymbol{K}[k]\boldsymbol{x}[k]$ where $\boldsymbol{K}[k]$ is called the gain matrix and is calculated using existing formulae from the literature. For nonlinear systems, an LQR-based optimization problem can be written by linearizing the system around an equilibrium point over the length of the horizon and regulating the difference between the actual state/input and the equilibrium state/input around the zero point which results in the control input trying to bring the system closer to the equilibrium states. In the context of traffic control, these equilibrium states and inputs are assigned values that result in an improvement in the state of traffic. In this case, the control input is defined by the following state-feedback law which takes into account the selected equilibrium states and inputs:

$$\boxed{\boldsymbol{u}[k] = -\boldsymbol{K}[k]\boldsymbol{x}[k] + \boldsymbol{u}^*[k] + \boldsymbol{K}[k]\boldsymbol{x}^*[k],} \tag{6}$$

where $\boldsymbol{K}[k] \in \mathbb{R}^{n_u \times n_x}$ and $(\boldsymbol{x}^*[k], \boldsymbol{u}^*[k])$ denote the time-varying LQR state-feedback matrix and the time-varying equilibrium point of the nonlinear system (4) at time index k, respectively.

To obtain the gain matrix $\boldsymbol{K}[k]$ at any time-step for controlling the nonlinear system within the LQR framework, the Gauss-Newton LQR (GN-LQR) algorithm [13] can be applied. The same is presented in the remainder of this section along with a variant of the GN-LQR algorithm that penalizes changes in control inputs over consecutive time-steps. Various parameters of these algorithms are investigated in the ensuing sections in the context of traffic control using moving bottlenecks.

A. The Gauss-Newton LQR (GN-LQR) algorithm

Here, we present an iterative LQR algorithm called the GN-LQR algorithm [13] which can be used to solve the LQR optimization problem (5) for the given nonlinear system (4). We introduce the following notation before presenting the GN-LQR algorithm:
N: horizon length.
N-step input and state matrices:

$$\begin{aligned} \boldsymbol{U} &:= \begin{bmatrix} \boldsymbol{u}[0] & \cdots & \boldsymbol{u}[N-1] \end{bmatrix}, \\ \boldsymbol{X} &:= \begin{bmatrix} \boldsymbol{x}[0] & \cdots & \boldsymbol{x}[N] \end{bmatrix}. \end{aligned}$$

Corresponding time-varying equilibrium counterparts:

$$\begin{aligned} \boldsymbol{U}^* &:= \begin{bmatrix} \boldsymbol{u}^*[0] & \cdots & \boldsymbol{u}^*[N-1] \end{bmatrix}, \\ \boldsymbol{X}^* &:= \begin{bmatrix} \boldsymbol{x}^*[0] & \cdots & \boldsymbol{x}^*[N] \end{bmatrix}. \end{aligned}$$

Corresponding control input difference matrix:

$$\boldsymbol{\delta U} := \begin{bmatrix} \boldsymbol{\delta u}[0] & \cdots & \boldsymbol{\delta u}[N-1] \end{bmatrix},$$

Linearized state-space matrices:

$$\hat{\boldsymbol{A}}[k] = \boldsymbol{A} + \boldsymbol{G}\boldsymbol{A}_{\boldsymbol{f}}[k],\ \hat{\boldsymbol{B}}[k] = \boldsymbol{G}\boldsymbol{B}_{\boldsymbol{f}}[k], \tag{7}$$

where
$\boldsymbol{A}_f[k]$: The derivative matrix of $\boldsymbol{f}(\boldsymbol{x}[k],\boldsymbol{u}[k])$ w.r.t. $\boldsymbol{x}^*[k]$,
$\boldsymbol{B}_{\boldsymbol{f}}[k]$: The derivative matrix of $\boldsymbol{f}(\boldsymbol{x}[k],\boldsymbol{u}[k])$ w.r.t. $\boldsymbol{u}^*[k]$.
The LQR cost function to be minimized:

$$J(\boldsymbol{x}[k],\boldsymbol{u}[k]) := J_x(\boldsymbol{x}[k]) + J_u(\boldsymbol{u}[k]), \tag{8}$$

where

$$J_x(\boldsymbol{x}[k]) := \sum_{k=0}^{N-1} (\boldsymbol{x}^*[k] + \boldsymbol{\delta x}[k])^T \boldsymbol{Q} (\boldsymbol{x}^*[k] + \boldsymbol{\delta x}[k]),$$

$\boldsymbol{Q}$: The LQR state-weight matrix, $\boldsymbol{Q} \succeq \boldsymbol{0}$,

$$J_u(\boldsymbol{u}[k]) := \sum_{k=0}^{N-1} (\boldsymbol{u}^*[k] + \boldsymbol{\delta u}[k])^T \boldsymbol{R} (\boldsymbol{x}^*[k] + \boldsymbol{\delta u}[k]),$$

$\boldsymbol{R}$: The LQR input-weight matrix, $\boldsymbol{R} \succ \boldsymbol{0}$.

The goal of the algorithm is to minimize the above objective function given the state-space dynamics (4) along with physical bounds on the speeds. The GN-LQR algorithm [13] can be summarized in Algorithm 1. To the standard algorithm, we also add a step to impose a non-negativity constraint and an upper bound on the speed equal to the free-flow speed.

B. The Gauss-Newton LQR algorithm with a penalty on variation in inputs

The controls produced at any time-step using the GN-LQR controller are independent of the controls in the previous time-steps. Due to this, the optimal controls can vary significantly over consecutive time-steps as is observed in Section IV. Since these controls are executed by CAV-platoons that are traveling within a traffic stream comprised of both autonomous and human-driven vehicles, the latter of which can sometimes have high reaction times, large changes in control inputs over consecutive time-steps can result in life-threatening collisions due to vehicles not braking in time. To avoid such circumstances, here we present a variant of the LQR optimization problem which applies a penalty on changes in control inputs over consecutive time-steps thus preventing large

Algorithm 1: The GN-LQR Algorithm

input: State-space matrices $\boldsymbol{A}$, $\boldsymbol{G}$, nonlinear function $\boldsymbol{f}$, initial state $\boldsymbol{x}[0]$, horizon length N, LQR weight matrices $\boldsymbol{Q}$, $\boldsymbol{R}$, error tolerance ϵ, maximum number of iterations M, initial guess for equilibrium control inputs $\boldsymbol{U}^*$, and initial guess for initial equilibrium state $\boldsymbol{x}^*[0]$.
set: current iterate $i=0$, $\boldsymbol{U}=\boldsymbol{U}^*$, $\boldsymbol{\delta U}=\boldsymbol{U}-\boldsymbol{U}^*$, $\boldsymbol{\delta x}[0]=\boldsymbol{x}[0]-\boldsymbol{x}^*[0]$.
repeat
  for $k=0,...,N-1$ **do**
    compute: $\hat{\boldsymbol{A}}[k],\hat{\boldsymbol{B}}[k]$ via (7) around the time-varying equilibrium point $(\boldsymbol{x}^*[k],\boldsymbol{u}^*[k])$ of nonlinear dynamics (4) at time index k.
    set: $\boldsymbol{\delta x}[k+1]=\hat{\boldsymbol{A}}[k]\boldsymbol{\delta x}[k]+\hat{\boldsymbol{B}}[k]\boldsymbol{\delta u}[k]$.
    compute: $\boldsymbol{x}^*[k+1]$ via nonlinear dynamics (4).
  ▷ Solve the Gauss-Newton optimization problem for controller gains $\boldsymbol{K}[0],...,\boldsymbol{K}[N-1]$
  set: $\boldsymbol{P}[N]=\boldsymbol{0}$
  for $l=N,...,1$ **do**
    set: $\boldsymbol{P}[l-1]=\boldsymbol{Q}+\hat{\boldsymbol{A}}[l-1]^T\boldsymbol{P}[l]\hat{\boldsymbol{A}}[l-1]-\hat{\boldsymbol{A}}[l-1]^T\boldsymbol{P}[l]\hat{\boldsymbol{B}}[l-1]\times(\boldsymbol{R}+\hat{\boldsymbol{B}}[l-1]^T\boldsymbol{P}[l]\hat{\boldsymbol{B}}[l-1])^{-1}\hat{\boldsymbol{B}}[l-1]^T\boldsymbol{P}[l]\hat{\boldsymbol{A}}[l-1]$.
  for $k=0,...,N-1$ **do**
    set: $\boldsymbol{K}[k]=(\boldsymbol{R}+\hat{\boldsymbol{B}}[k]^T\boldsymbol{P}[k+1]\hat{\boldsymbol{B}}[k])^{-1}\hat{\boldsymbol{B}}[k]^T\boldsymbol{P}[k+1]\hat{\boldsymbol{A}}[k]$.
    set: $\boldsymbol{\delta u}[k]=-\boldsymbol{K}[k]\boldsymbol{\delta x}[k]$.
  set: $\boldsymbol{\delta U}=\begin{bmatrix}\boldsymbol{\delta u}[0] & \cdots & \boldsymbol{\delta u}[N-1]\end{bmatrix}$
  set: $\boldsymbol{U}=\min\{\max\{\boldsymbol{U}^*+\boldsymbol{\delta U},0\},v_f\}$, $\boldsymbol{U}^*=\boldsymbol{U}$, $i=i+1$.
until $\|\boldsymbol{\delta U}\|<\epsilon$ *or* $i>M$
compute: $\boldsymbol{u}[0]$ via (6) using $\boldsymbol{K}[0]$.
output: $\boldsymbol{u}[0]$.

changes in control inputs. The implementation of the optimization problem is derived based on [14] which prescribes the inclusion of an additional term in the LQR objective function penalizing variations in control inputs. This is achieved by modifying the state-space formulation of the system by defining a new state which is an augmentation of the original state vector and the original control input vector and a new control input vector that captures the change in control input. A new weight matrix $\boldsymbol{R}'$ is introduced in the LQR optimization problem that governs the fluctuations in the control inputs. A larger magnitude of elements in $\boldsymbol{R}'$ implies a larger penalty on the change in control inputs over consecutive time-steps whereas $\boldsymbol{R}'=\boldsymbol{0}$ implies no penalty is imposed. The GN-LQR algorithm presented in the previous section can be modified to obtain the new algorithm which is referred to as GN-LQR-with-penalty (GN-LQRP) in the remainder of the paper and is omitted for brevity. More details on the same can be found in [12].

IV. Numerical Study And Implementation

In this section, we investigate the performance of the proposed control algorithms for moving bottleneck-based traffic control with the help of a macroscopic simulation and compare it with existing PI- [4] and MPC-based [5] controllers. This is followed by a microsimulation-based case study using the Transmodeler 6.1 [15], [16] traffic simulation software to test the near real-world performance of the controller and to learn the advantages and gaps in applying the controller in the real world. All macroscopic simulations applying the CTM model are performed using MATLAB R2021b running on a 64-bit Windows 10 with a 2.2GHz IntelR CoreTM i7-8750H CPU and 16GB of RAM while the microscopic simulations are performed on a 64-bit Windows 10 with a 2.3GHz IntelR CoreTM i7-11800H CPU and 16GB of RAM.

A. Scenario description and evaluation metrics

The traffic is modeled using the dynamics presented in Section II. We consider an 8 km long highway stretch with no on-ramps or off-ramps which is divided into 16 even segments of length 0.5 km each. A total duration of 2 hr is considered for the example with time divided into steps of the duration of 10 sec each. The following values of traffic flow parameters are used for the fundamental diagram considered in this work [12]: critical density $\rho_c = 60$ veh/km, free-flow speed $v_f = 100$ km/hr, congestion wave speed $w_c = 38$ km/hr, maximum density $\rho_m = 320$ veh/km, maximum flow $q^{\text{cap}} = 6000$ veh/hr, and capacity drop parameter $\alpha = 0.83$, similar to [5]. We consider a platoon length of 4.5 m which essentially implies platoons of one CAV per lane, and $S_{min} = 10$. The initial density on all the segments is set to 20 veh/km. The supply available at the downstream end of the highway is set to q^{cap} while the demand wanting to enter at the upstream end of the highway starts and ends at 1900 veh/hr with a value of 5490 veh/hr from 120 to 600 seconds. A reduced flow area is simulated on the highway by reducing the outflow of Segment 13 to 5400 veh/hr for the first hour after which the flow of the segment is restored to maximum capacity. The impact of the control is measured using three metrics, the Total Travel Time (TTT) in veh·hr, the Total Travel Distance (TTD) in veh·km, and the Mean Speed (MS) in km/hr which are defined similarly to [5] as follows:

$$\text{TTT} := TL\sum_{k=1}^{N_T}\sum_{i=1}^{N_L}\rho_i[k],\ \text{TTD} := TL\sum_{k=1}^{N_T}\sum_{i=1}^{N_L}\phi_i[k],\ \text{and}$$
$$\text{MS} := \text{TTD}/\text{TTT}.$$

where T, L, N_T, and N_L are the duration of each time-step, the length of each segment, the total number of time-steps in the simulation, and the total number of segments in the considered highway stretch, respectively. In general, a lower TTT, a higher TTD, and a higher MS are desirable — The closer the traffic density is to the critical density, the better the values of these metrics as the traffic is free-flowing and at the maximum flow possible. Therefore, at each implementation of the LQR-based controllers we select such equilibrium states for linearization which improves the values of these metrics. Besides these metrics, we also consider the Average Computation Time (ACT) for each controller which is defined as the average time required to compute the control inputs at any time-step during the simulation. We assume that controlled vehicles enter the stretch every 15 time-steps starting from time-step 60 to time-step 600 of the process horizon. Figure 2 presents the simulated traffic densities in the presence of the reduced flow and without any control implementation. The metrics for this case are presented in Table I.

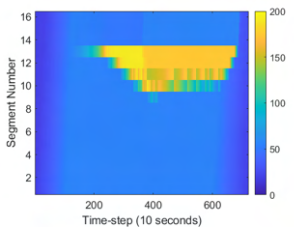

Fig. 2. Density (veh/km) evolution in the uncontrolled case with the reduced bottleneck flow.

B. A note on proposed controller tuning

Analysis of the tuning is omitted from this paper for brevity and only important results are presented. Interested readers are referred to [12] for detailed analysis related to tuning of the proposed controller parameters. In this work, $N=3$ is chosen for GN-LQR while $N=50$ is chosen for GN-LQRP. Regarding the maximum number of iterations, it is observed that the best performance of the GN-LQR controller is achieved at the number of iterations = 1. For this analysis, the LQR objective weight matrices are defined as diagonal matrices in the form $\boldsymbol{Q} = \begin{bmatrix} w_Q \boldsymbol{I}_{\boldsymbol{N_L}} & \boldsymbol{0} \\ \boldsymbol{0} & \boldsymbol{0}_{N_{\text{CAV}}} \end{bmatrix}$, $\boldsymbol{R} = w_R \boldsymbol{I}_{N_{\text{CAV}}}$, and $\boldsymbol{R'} = w_{R'} \boldsymbol{I}_{N_{\text{CAV}}}$ where $w_Q, w_R, w_{R'} \in \mathbb{R}$. It is observed that a larger magnitude of w_Q compared with w_R results in a better performance. Also, increasing the magnitude of $w_{R'}$, naturally results in further degradation in the performance as the reduction in speeds is further restricted. The values $w_Q = 100$, $w_R = 1$, and $w_{R'} = 30$ are found suitable in this study. Additionally, the equilibrium density is set to 59 veh/km and the equilibrium speed is set to 99 km/hr. The values are set a little below ρ_c and v_f to allow for Jacobian calculation which requires a small perturbation of solutions around the equilibrium solution.

C. Comparison of GN-LQR and GN-LQRP with PI- and MPC-based controllers

Here, we present the results obtained from using the proposed algorithms and compare them with those obtained from using the PI- and MPC-based controllers which are implemented the same as in [4] and [5], respectively. Table I presents the values of the evaluation metrics for all controller implementations for the given scenario. It is observed that the GN-LQR and GN-LQRP algorithms result in a significant improvement over the uncontrolled scenario. The density evolution plots are presented in Figure 3. The improvement is achieved by creating smaller controlled reductions in segment flows (by reducing the CAV-platoon speeds) upstream of the bottleneck segment (Segment 13). Since the outflow of segments decreases with an increase in density above ρ_c, reducing the flow of traffic in small amounts in the upstream segments thereby increasing their density in small amounts while preventing higher densities in the bottleneck segments results in overall higher flows across all the segments. This is the underlying idea behind moving bottleneck control which is correctly executed by the LQR-based controllers. For the PI-based controllers, we obtain optimal gains for the given scenario by setting up a nonlinear optimization problem with the objective of maximizing the MS. For the MPC-based controller the weights and horizon length are set the same as in [5]. The studies [4], [5] also prescribe a lower bound of 60 km/hr for the control speed to account for a low reaction time of human

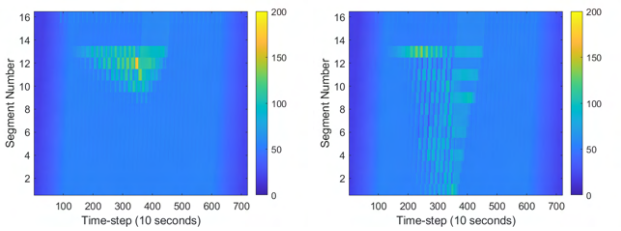

Fig. 3. Density (veh/km) evolution on the highway stretch with [left] GN-LQR and [right] GN-LQRP controllers.

TABLE I

EVALUATION METRICS WITH DIFFERENT CONTROLLERS.

Scenario	TTT	TTD	MS	CT
No Control	1,019.0	78,998	77.5	-
PI (lower bound 60 km/hr)	820.8	78,741	**95.9**	7.1051
PI (no lower bound)	1,017.5	78,741	77.3	1.5982
MPC (lower bound 60 km/hr)	840.6	78,741	93.6	2.8729
MPC (no lower bound)	848.7	78,741	92.7	3.3722
GN-LQR ($N=3$)	832.5	78,741	94.5	**0.0058**
GN-LQRP ($R'=30\boldsymbol{I}, N=50$)	839.7	78,741	93.7	0.0884

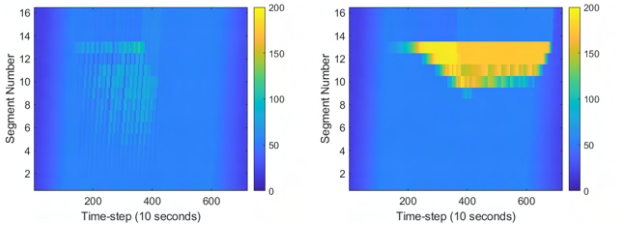

Fig. 4. Density (veh/km) evolution on the highway stretch with PI-based control with an [left] optimal gains and lower bound of 60 km/hr, and [right] optimal gains and no lower bound.

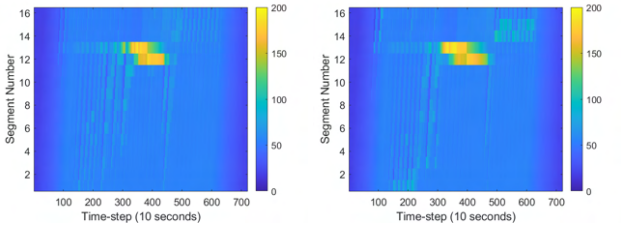

Fig. 5. Density (veh/km) evolution on the highway stretch with MPC-based control with a [left] lower bound of 60 km/hr, and [right] no lower bound.

drivers and prevent accidents due to sudden speed drops. This is implemented by projecting the controller speed to the bounds. However, with increased connectivity and autonomy in vehicles, it is possible to expect no plausible limit to what the speeds can be dropped to. In this study, we, therefore, also test the controllers with and without a lower bound on the speed.

Figures 4 and 5 present the density evolution plots for the PI- and MPC-based controllers with and without a lower bound. The PI-based controller with a lower bound reduces the impact of the bottleneck while the controller without a lower bound, results in no improvement in the MS over the uncontrolled case. In the second case, the best value of the gains that minimize the controller error, results in blocking all the vehicles at the upstream end but this results in a small MS and hence the gains selected in this case are such that the controller does not affect the traffic conditions at all. The MPC-based controller results in an improvement in the traffic condition in both cases. To assess the speed variation using the different controllers we present the speed profile of CAV-platoon 11

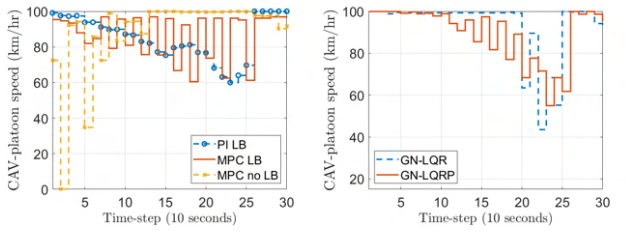

Fig. 6. CAV-platoon speed profile for platoon 11 with [left] PI-based controller with a lower bound, and MPC-based controller with and without lower bound, and [right] GN-LQR controller and GN-LQRP controller with $\boldsymbol{R}' = 30\boldsymbol{I}$.

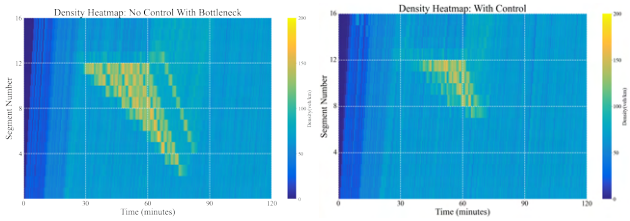

Fig. 7. Density (veh/km) evolution on the highway stretch in microsimulation for the different scenarios: [left] no control with bottleneck, [right] with control.

TABLE II

METRICS FOR SCENARIOS TESTED IN THE MICROSIMULATION

Scenarios	TTT	TTD	MS
No bottleneck	949	78,708	82.94
No control with bottleneck	1,059	78,724	74.34
GN-LQR-based control with bottleneck	991	79,333	80.05

that enters the highway at time-step 210 in Figure 6. The speed profiles for the PI-based and the GN-LQRP controllers are observed to be the smoothest with a gradual reduction in speeds. The GN-LQR and the MPC-based controller without a lower bound result in large abrupt changes in speeds for the platoon within a time-step. Theoretically, such variations in speed are possible within a time-step (which is equal to 10 seconds) however, they can be unsafe under high reaction times. While the MPC-based controller with a lower bound prevents as high of speed fluctuations as in the GN-LQR and MPC-based without a bound, we can still observe fluctuations close to 40 km/hr which is the shift from the maximum speed to the lower bound value. This shows that the lower fluctuations are not a property of the controller (as in the case of GN-LQRP) but an artifact of the lower bound which is arbitrarily imposed.

Table I also presents the computation time (CT) in seconds for all the controllers which refers to the ACT in the case of MPC- and LQR-based controllers and to the offline computation time for gain calculation in the case of PI-based controllers. In the current work, the PI-based controller only requires offline gain computation and there is virtually no real-time computation time for the controller. Although in cases when the offline gains do not work as expected due to different realization of the traffic conditions than expected, then real-time computation of gains may be required. The CT for the LQR-based controllers mostly comprises the time to compute the derivatives of the state space equation with respect to the equilibrium states and inputs and is almost two orders of magnitude smaller than the CT for the MPC-based controllers.

V. MICROSIMULATION CASE STUDY

In this section, we reproduce the traffic control scenario using a realistic microscopic traffic simulator and use it to test the performance of the GN-LQR control algorithm under a realistic setting. The micro-simulation is performed using TransModeler 6.1 [15], [16] while the control algorithm is implemented using MATLAB R2021b. The GISDK API in TransModeler is used to interact with the controller.

A. Simulation setup

The setup of the highway stretch and the traffic demands are consistent with the traffic scenario presented in Section IV. The highway stretch is designed with three lanes with a maximum capacity of 2000 veh/hr/lane. A bottleneck is generated by a work zone (a lane-changing guide signal with a 30% compliance rate) on Segment 13. The microscopic simulation parameters are carefully tuned to reproduce the bottleneck and the capacity drop which are consistent with the scenario described in Section IV.

The CAV-platoons consist of three vehicles traveling side-by-side acting as rolling roadblocks trying to block all traffic behind them and not allowing any vehicles to pass by. These CAV-platoons enter the network every 150 seconds. Note that there are three different update frequencies used in the microsimulation namely the simulation step update frequency which is 10Hz, the state variables and controller update frequency which is 0.1Hz, and the controlled CAV-platoon speed update frequency is 1Hz. The traffic densities across the highway stretch and the position of the CAV-platoons on the stretch at the current time-step are obtained from the microsimulation and passed to the GN-LQR controller (Algorithm 1) which prescribes control speeds to the CAV-platoons on the stretch. The other inputs to the controller are obtained from the CTM model described in Section II.

B. Simulation result

Table II presents the values of the evaluation metrics obtained from the microscopic traffic simulation both in the presence and absence of a bottleneck on the highway as well as in the case in which control is implemented using the GN-LQR algorithm to mitigate the impact of the bottleneck. Figure 7 presents the density evolution plots with a bottleneck both with and without control. It is observed that the GN-LQR algorithm results in an improvement in MS compared to the uncontrolled scenario. In the controlled scenario, TTD is increased due to the extra CAV-platoons (36 platoons and 108 vehicles in total) sent into the highway stretch. The TTT is reduced using the LQR-based controller compared to the uncontrolled scenario. In the controlled case, the size of the jam created by the bottleneck is reduced in both space and time as the congestion wave propagates over a smaller duration. Figure 8 presents a space-time diagram of the trajectories of all vehicles over the simulation duration, with the red lines indicating the trajectories of the CAV-platoons. Observing the trajectories of the platoons along with their impact on the surrounding traffic provides further insights into the performance of the controller. It is seen that the improvement is achieved by slowing down the vehicles about to join the jam thus creating larger gaps behind the jam that allow for the congestion wave to dissipate (see Figure 8 zoomed-in area for more details). The jams created by this slowing down of vehicles behind the existing jam are rather small and dissipate on their own or with the help of gaps created by the CAV-platoons that follow. This is similar to the observations made in the case of the macroscopic

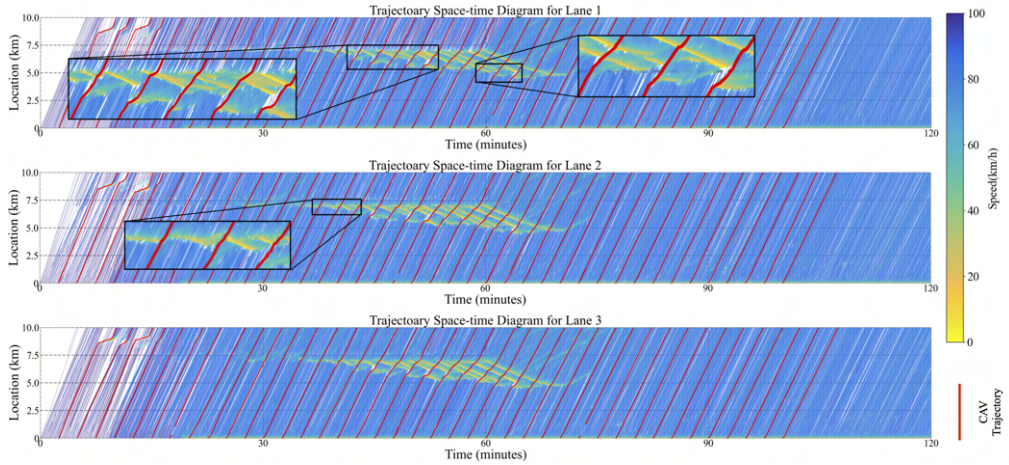

Fig. 8. Vehicle trajectory space-time diagram for the controlled scenario (the color of each trajectory point reflects the speed of the vehicle at the time, and the CAV-platoons trajectories are labeled with red lines): [top] the left lane, [middle] the middle lane, [bottom] the right lane.

simulation-based analysis and provides preliminary confirmation of the usability of the controller in a realistic setting. Interested readers are referred to [12] for results related to the implementation of the other controllers in a microscopic simulation setting.

VI. Conclusions and Future Direction

From the above analysis, it is observed that both GN-LQR and GN-LQRP controllers are able to reduce the negative effects of fixed bottlenecks on the highway stretch. The performance of the GN-LQR controller is comparable to the MPC-based controller (with and without lower bound on control speeds) and the PI-based controller (with lower bound on control speeds) at small values of N while the performance of GN-LQRP is comparable to the other controllers at a larger $N = 50$. The PI-based controller without a lower bound on the control speed does not improve the condition of traffic. Both LQR-based controllers outperform the MPC-based controller in terms of computation time for each controller run. Based on obtained results, LQR-based controllers are almost two orders of magnitude faster than the MPC-based controller. The PI-based controller is the fastest as it only requires the offline computation of the gains. However, this is contingent upon the existence of a reliable way to compute the gains offline. The controls obtained from all the controllers are plausible in terms of maximum acceleration/deceleration requirements for vehicles to achieve the prescribed speeds. However, accounting for human reaction times, the PI-based controller (with a lower bound on the control speed) and the GN-LQRP controller offer the safest and most realistically achievable controls. In the microsimulation-based study, the LQR-based controller is observed to improve the traffic conditions compared to the uncontrolled scenario resulting in a reduction in the size of the jam created by the bottleneck on the highway stretch.

Future directions of this work include the extension to large-scale road networks with the incorporation of junctions. Other forms of control such as ramp metering and variable speed limits can also be tested for incorporation into the current framework by considering the corresponding controls as inputs to the system thus allowing for integrated control. Also, robust control with unknown parameters in the realistic setting remains unsolved for this control problem and can be explored by testing and evaluating more scenarios in microsimulation.

References

[1] M. L. Delle Monache, J. Sprinkle, R. Vasudevan, and D. Work, "Autonomous vehicles: From vehicular control to traffic control," in *IEEE 58th Conference on Decision and Control (CDC)*. IEEE, 2019, pp. 4680–4696.

[2] H. Liu, L. Zhang, D. Sun, and D. Wang, "Optimize the settings of variable speed limit system to improve the performance of freeway traffic," *IEEE Transactions on Intelligent Transportation Systems*, vol. 16, no. 6, pp. 3249–3257, 2015.

[3] P. Goatin, S. Göttlich, and O. Kolb, "Speed limit and ramp meter control for traffic flow networks," *Engineering Optimization*, vol. 48, no. 7, pp. 1121–1144, 2016.

[4] G. Piacentini, C. Pasquale, S. Sacone, S. Siri, and A. Ferrara, "Multiple moving bottlenecks for traffic control in freeway systems," in *18th European Control Conference (ECC)*. IEEE, 2019, pp. 3662–3667.

[5] G. Piacentini, A. Ferrara, I. Papamichail, and M. Papageorgiou, "Highway traffic control with moving bottlenecks of connected and automated vehicles for travel time reduction," in *IEEE 58th Conference on Decision and Control (CDC)*, 2019, pp. 3140–3145.

[6] M. J. Lighthill and G. B. Whitham, "On kinematic waves ii. a theory of traffic flow on long crowded roads," *Proceedings of the Royal Society of London. Series A. Mathematical and Physical Sciences*, vol. 229, no. 1178, pp. 317–345, 1955.

[7] P. I. Richards, "Shock waves on the highway," *Operations Research*, vol. 4, no. 1, pp. 42–51, 1956.

[8] K. Yuan, V. L. Knoop, and S. P. Hoogendoorn, "Capacity drop: Relationship between speed in congestion and the queue discharge rate," *Transportation Research Record*, vol. 2491, no. 1, pp. 72–80, 2015.

[9] S. K. Godunov, "A difference method for numerical calculation of discontinuous solutions of the equations of hydrodynamics," *Matematicheskii Sbornik*, vol. 89, no. 3, pp. 271–306, 1959.

[10] C. F. Daganzo, "The cell transmission model: A dynamic representation of highway traffic consistent with the hydrodynamic theory," *Transportation Research Part B: Methodological*, vol. 28, no. 4, pp. 269–287, 1994.

[11] R. Courant, K. Friedrichs, and H. Lewy, "On the partial difference equations of mathematical physics," *IBM journal of Research and Development*, vol. 11, no. 2, pp. 215–234, 1967.

[12] S. C. Vishnoi, J. Ji, M. Bahavarnia, Y. Zhang, A. F. Taha, C. G. Claudel, and D. B. Work, "CAV traffic control to mitigate the impact of congestion from bottlenecks: A linear quadratic regulator approach and microsimulation study," 2023.

[13] S. Boyd, "Linear quadratic regulator: Discrete-time finite horizon, lecture notes," 2008.

[14] P. Abbeel, "Optimal control for linear dynamical systems and quadratic cost, lecture notes," 2012.

[15] Q. Yang and H. N. Koutsopoulos, "A microscopic traffic simulator for evaluation of dynamic traffic management systems," *Transportation Research Part C: Emerging Technologies*, vol. 4, no. 3, pp. 113–129, 1996.

[16] R. Balakrishna, D. Morgan, H. Slavin, and Q. Yang, "Large-scale traffic simulation tools for planning and operations management," *IFAC Proceedings Volumes*, vol. 42, no. 15, pp. 117–122, 2009.